Preprint
UCRL-JC-149593

Longitudinal Coherence Measurements of the Transient Collisional X-ray Laser

R. F. Smith, S. Hubert, M. Fajardo, P. Zeitoun, J. Dunn, J. R. Hunter, C. Remond, L. Vanbostal, S. Jaquemot, J. Nilsen, C. L. S. Lewis, R. Marmoret

This article was submitted to
18th International Conference on X-ray Lasers, Aspen, CO., May 27-31, 2002

U.S. Department of Energy

Lawrence Livermore National Laboratory

August 9, 2002

This work was performed under the auspices of the United States Department of Energy by the University of California, Lawrence Livermore National Laboratory under contract No. W-7405-Eng-48.

Longitudinal Coherence Measurements of the Transient Collisional X-ray Laser

Raymond F. Smith[1], Sebastian Hubert[3], Marta Fajardo[2], Philippe Zeitoun[2], James Dunn[1], James R. Hunter[1], Christian Remond[3], Laurent Vanbostal[2], Silvie Jaquemot[3], Joseph Nilsen[1], Ciaran L.S. Lewis[4], Remy Marmoret[3]

[1]Lawrence Livermore National Laboratory, Livermore, CA 94551
[2]Laboratoire d'Interaction du rayonnement X avec la Matiére (LIXAM), Université Paris-Sud, Bât 350, 91405 Orsay, France.
[3]Commisariat á l'Ènergie Atomique, BP 2, 91680 Bruyeres-le-Chatel, France.
[4]School of Mathematics and Physics, The Queen's University of Belfast, Belfast BT7 1NN, UK.

Abstract. The first longitudinal coherence measurement of the transient inversion collisional x-ray laser is presented. The scheme underst udy is the picosecond output of the Ni-like Pd x-ray laser at 14.68 nm generated by the COMET laser facility at LLNL. Interference fringes were generated using a Michelson interferometer setup in which a thin multilayer membrane was used as a beam splitter. Longitudinal coherence measurements were made for this transition by changing the length of one interferometer arm and measuring the resultant variation in fringe visibility. The nature of this dependence also allows for an estimation of the linewidth of the lasing transition to be made. Analysis indicates a linewidth of ~0.3 pm which is a factor of four less than previous measurements on quasi-steady state x-ray laser schemes.

1. INTRODUCTION

The rapid development of x-ray lasers in recent years combined with the availability of optics in the XUV has led to several applications, such as interferometry [1] and holography [2], which depend on the coherence properties of the source pulse. Accurate measurements of the longitudinal coherence are important for determining feasibility and design parameters of instrumentation for such experiments. The longitudinal coherence is quantitatively related to the spectral bandwidth, $\Delta\lambda$, of the source and is a measure of the temporal separation along a beam in which the different spectral components maintain a phase relationship. In amplitude division interferometry the phase front of one arm is spatially overlapped and co-propagated with the other arm at the output of the interferometer. If the arm lengths are equalized to an accuracy better than the coherence length, L_c, of the source, interference fringes will be generated. The additional measurement of the spectral linewidth provides valuable insights into the gain dynamics within the lasing medium.

Saturated lasing at XUV wavelengths is typically generated through single pass amplification along an extended laser-produced plasma column. Previous experimental measurements of L_c have been made on the NOVA generated Ne-like Y x-ray laser at 15.5 nm [3]. This lasing scheme was generated with a 350 ps pulse, which generated a quasi-steady state population inversion on the main lasing transition. The duration of the x-ray laser pulse was comparable to the pulse width of the optical driver with gain conditions ultimately extinguished through plasma expansion and radiative cooling. The longitudinal coherence of this lasing scheme was measured to be ~100 μm, using a Mach-Zehnder type interferometer [3] of a long ~ns prepulse with a short ~ps main heating pulse. A large population inversion is created for a period before collisional redistribution of the excited state populations can take place. The attractiveness of this lasing scheme lies in the picosecond output, which makes it particularly suitable for characterizing fast evolving events. With this paper we present the first measurements of the longitudinal coherence of the transient collisional x-ray laser.

2. EXPERIMENTAL SETUP

The Ni-like Pd 14.7 nm x-ray laser probe beam was generated using two laser beams at 1054 nm wavelength from the COMET facility at LLNL [5]. Single pass saturated x-ray laser output of a few 10's of μJs was achieved with an optical pumping combination of a 600 ps long pulse (2 J, 2×10^{11} W cm^{-2}) and a 13 ps (5 J, 3×10^{13} W cm^{-2}) main heating pulse [6]. Traveling wave irradiation using a 7-step reflection echelon along the 1.6 cm line focus geometry was employed on a 1.25 cm polished slab Pd target to produce amplification in the axial direction. Approximately ten shots can be taken on the same target position before the output of the x-ray laser degrades significantly. Over the lifetime of a target position the output mode structure of the x-ray laser was found to be repeatable.

The x-ray laser output was imaged (Figure 1) and partially collimated by a normal incidence Mo/Si multilayer spherical mirror (S1), with $f = 11.75$ cm, and routed via a 45° multilayer mirror, to the input path of the Michelson interferometer. The measured reflectivity (assuming unpolarized light) of these two Mo/Si multilayer optics was 0.62 (S1) and 0.30 at the laser wavelength with a bandpass of 0.62 nm and 1.44 nm, respectively. The x-ray laser pointing stability along the input path of the interferometer was better than 100 μm from shot-to-shot. Upon entering the interferometer the x-ray laser beam interacts with a thin foil beamsplitter (BS), which is partially transmissive and partially reflective at the 14.7 nm wavelength. The beamsplitter consists of a 89nm thick Si_3N_4 membrane (0.5×0.5 cm^2) coated either side with 4.5 bi-layers of Mo/Si. The reflectivity at the x-ray laser wavelength is 14.4 % with a bandwidth of 2.7 nm.

One arm of the interferometer is directed to 0° multilayer optic, M1, via a reflection from BS. The beam is then returned along the same optical path and is transmitted through the beamsplitter. The other interferometer arm, which is initially transmitted through BS, reflects off the 0° mirror M2 and reflects off BS to the output collection optics. Both arms are co-propagating after the beamsplitter en route to M3. If sufficient spatial and temporal overlap of the two arms is achieved interference fringes will be generated. The two arms of the interferometer (BS→M1, BS→M2) were set to have the same nominal length with a mechanical alignment rod, to an estimated accuracy of ~100 μm. Rough spatial overlap of the two arms was done using a charged coupled device camera (CCD1) placed before the imaging system (Fig. 1). Optimization of the spatial overlap is possible under vacuum with remote adjustment of the M2 tilt stage.

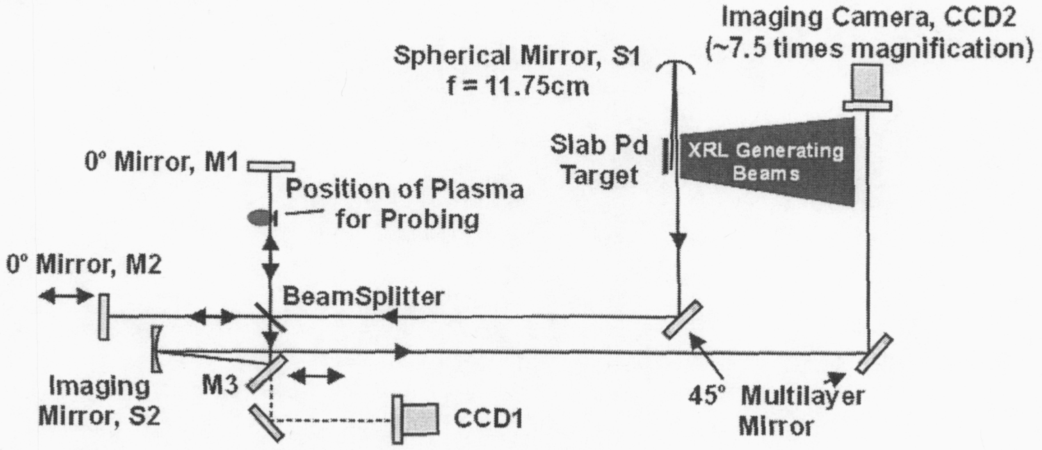

Figure 1. Setup for Michelson Interferometer Experiment.

The output signal from the interferometer reflects off M3 onto a spherical multilayer imaging mirror, S2, which has a focal length of 50 cm. The signal is routed from the imaging optic, via a 45° multilayer optic, to a thinned back-illuminated CCD2 detector with a 1024×1024 24 μm^2 pixel array. A 2000 Å Zr/1000 Å Polyimide ($C_{22}H_{10}N_2O_5$) filter was placed in front of the CCD to block visible and UV light. The imaging mirror was set to image the output plane of an Al target, within the M1 arm, from which a secondary plasma can be generated for pump-probe experiments. The total magnification of the imaging system was estimated to be ~7.5 giving a pixel limited resolution of 3.2 μm at the target plane. The reflectivity of the multilayered mirrors in the interferometer (also M3 and S2) is measured to be ~35% at the x-ray laser wavelength (s-polarization). The throughput of the interferometer is approximately 0.014.

Alignment of all the optics within the interferometer was done with the aid of a telescope, placed in the CCD2 camera position, and set on axis with the aid of alignment crosshair fiducials. A 5 mW HeNe diode laser was injected into the entrance aperture of the telescope. Absolute positioning of the optics tilt stages was achieved by retro-reflection of the HeNe alignment beam, off a given optic, back down to the telescope entrance aperture (autocollimation).

A sample interferogram is shown in Fig. 2 (a). The image captured by the CCD2 camera represents a region of ~1700 x 1700 μm^2 at the target plane. The curvature associated with the fringes is due to stresses across the beamsplitter causing local variations in the angles of the phase front within the x-ray beam. Figure 2(b) shows an integrated lineout (over box in 3(a)) which illustrated good levels of coherence across several hundred microns. Fringe visibilities, $V = (I_{max} - I_{min})/(I_{max} + I_{min})$, up to 70% have been measured. The large scale intensity variations across the image are due to mode structure within the x-ray laser. It has been observed that after equalization of the arms is achieved, there exists good coherent relationship between the modes. Structure along individual fringes may be due to non-uniformities within the beamsplitter or multilayer optics.

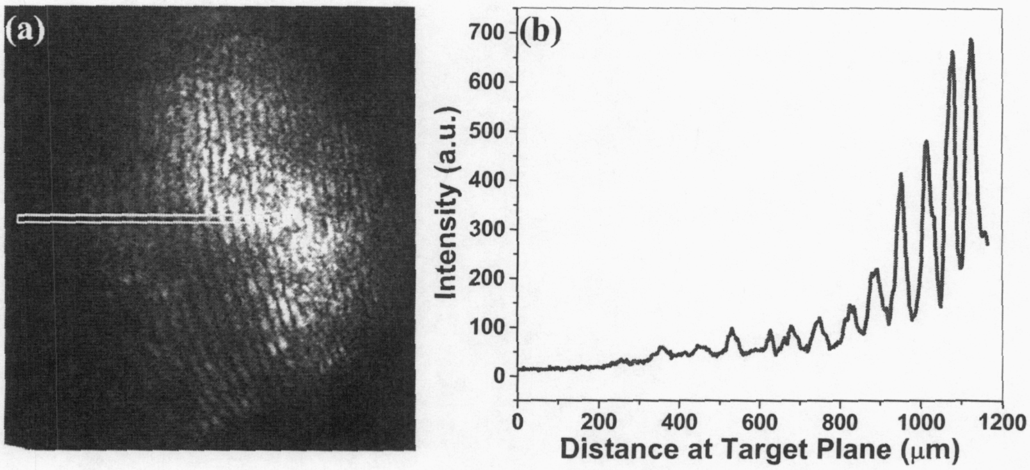

Figure 2 (a) Interferogram taken at ΔL = 0 for a 13 ps CPA heating pulse (b) Integrated lineout over box in (a) shows good visibility over several hundred microns.

3. LONGITUDINAL COHERENCE MEASUREMENTS

To determine the longitudinal coherence of the source the differential path length between the two arms of the interferometer was systematically varied and the fringe visibility in the interferograms monitored. This was achieved by incrementing the M2→BS length with encoded translation of M2 while keeping the distance from the beamsplitter to M1 fixed (Fig. 3). At least two shots were taken at each position to ensure repeatability. Each interferogram can be characterized in a number of ways: overall fringe continuity, number of adjacent fringes, number of counts on CCD, uniformity of intensity along a fringe and visibility. Sufficient quality must be achieved in all of these categories to ensure the interferogram is suitable for plasma probing experiments. It was found that there existed a high degree of speckle in the x-ray intensity pattern which was considered to be unrelated to the larger scale intensity variations associated with the inherent transverse mode structure of the x-ray laser. This speckle, which is possibly a result of inhomogeneities within the beamsplitter, was superimposed onto the interferograms giving rise to random high spatial frequencies in the intensity of the fringes. To obtain visibility measurements intensity averaging was carried out over a 30-pixel region, which is equivalent to 225 μm at the target plane. This had the effect of negating the speckle contribution whilst maintaining the accuracy of the visibility measurement. The results are shown in Fig.

3(b). Each data point signifies the average of nine measurements across a single interferogram. Ideally fringe visibilities up to 100% would be observed. In practice this was not achieved due to a small degree of spatial misalignment and slight variations between the optics. It was observed that for shots with increasing distance away from the nominal overlap position the regions over which fringes were visible became smaller. This may be due to adjacent transverse modes in the x-ray laser profile with, for example, the same coherence length but being temporally offset. Fringe visibilities below 0.2 were difficult to measure because at larger values of ΔL the fringe continuity was on a scale less than that of the integration window. Also shown in a Gaussian fit to the data points with the 1/e half-width yielding a coherence length measurement of 400 μm ± 35 μm. This is equivalent to a temporal coherence, τ_c, of ~1.33 ps.

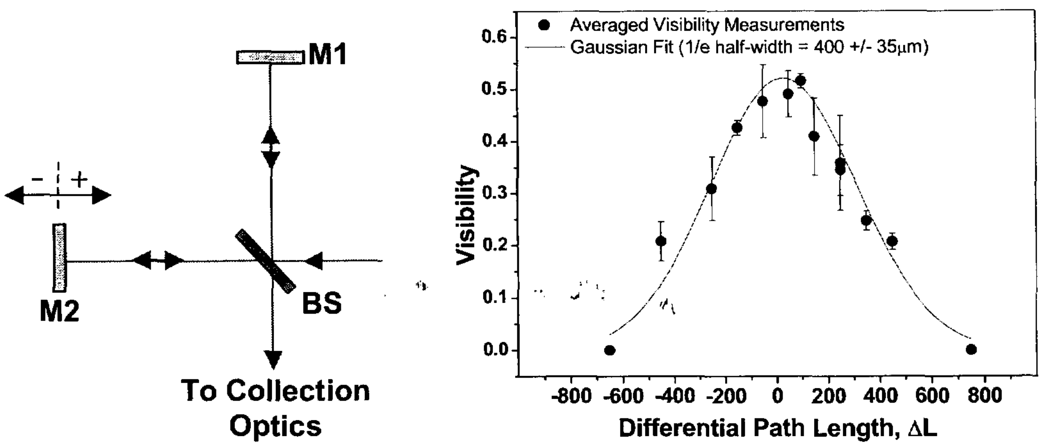

Figure 3. Variation of fringe visibility with path difference between two arms of the interferometer. Each data point represents the average visibility for a given shot taken from nine separate measurements across the interferogram. Standard deviations are shown via the error bars. Also shown is the best fit Gaussian curve with a 1/e half width of ~400 μm ± 35 μm.

Following [4] the measured fringe visibility is equal to the magnitude of the complex degree of coherence within the illumination beam. The latter is a measure of the degree of correlation between the two combining phase fronts at the output of the interferometer. By incrementing the length of the M2 arm by a distance L the phase front associated with that arm is delayed by a time τ = 2L/c. By using a Fourier transform relationship (Wiener-Khintchine theorem) the complex degree of coherence is shown to be related to the power spectral density of the x-ray laser pulse, $I(\upsilon)$. As a result of this relationship, the linewidth $\Delta\upsilon$ and the coherence time τ_c are inversely related. We assume the x-ray laser line has a Gaussian power spectrum such that,

$$I(\upsilon) \propto \exp\left[-2\sqrt{\ln(2)}\left(\frac{\upsilon-\upsilon_0}{\Delta\upsilon}\right)^2\right], \qquad (1)$$

where $\Delta\upsilon$ is the linewidth of the lasing transition, $\upsilon_0 = c/\lambda$. The measured fringe visibility dependence on τ, $V(\tau)$, is the envelope of the autocorrelation function of the power spectrum varying as,

$$V(\tau) = \exp\left[-\left(\frac{\pi\Delta\upsilon\tau}{2\sqrt{\ln 2}}\right)^2\right]. \tag{2}$$

The coherence time, τ_c, is defined as the value of τ at which the visibility has decreased to 1/e the maximum value. From figure 4(b) we have a $\tau_c \sim 1.33 \pm 0.12$ ps, which yields an equivalent Gaussian FWHM linewidth of 0.29 ± 0.03 pm. For an expected ion temperature of 80eV [5] within the gain medium the Doppler broadened lineshape would be equivalent to ~1 pm. Our lower measurement of ~0.3 pm is an expected result of gain narrowing effects. The measured linewidth is a factor of four less than the 1.3 pm previously measured for the Ni-like Y quasi-state state x-ray laser scheme [3]. In that work the predicted ion temperature was 600eV, which gave rise to enhanced levels of Doppler broadening.

ACKNOWLEDGEMENTS

The support of Al Osterheld and Andy Hazi is greatly appreciated. This work was performed under the auspices of the U.S. Dept. of Energy by the University of California Lawrence Livermore National Laboratory, under Contract No. W-7405-Eng-48. The optics used in the interferometer were funded through the CEA, France.

REFERENCES

1. L. B. Da Silva, T. W. Barbee, Jr., R. Cauble, P. Celliers, D. Ciarlo, S. Libby, R. A. London, D. Matthews, S. Mrowka, J. C. Moreno, D. Ress, J. E. Trebes, A. S. Wan, and F. Weber, Phys. Rev. Lett. **74**, 3991-3994 (1995); R.F. Smith, J.Dunn, J. Nilsen, V.N. Shlyaptsev, S. Moon, J. Filevich, J.J. Rocca, M.C. Marconi, J.R. Hunter, and T.W. Barbee, Jr., Phys. Rev. Lett., **89** (6), 065004-1 (2002).
2. J.E. Trebes, S.B. Brown, E.M. Campbell, D.L. Matthews, D.G. Nilson, G.F. Stone, D.A. Whelan, Science, **238** (4826), p.517 (1987); B. Rus, H. Daido, H. Tang, M. Nishiuchi, M. Kishimoto, M. Tanaka, T. Kawachi, N. Hasegawa, K. Nagahima,T. Arisawa, Y. Kato, , *these proceedings*.
3. P. Celliers, F. Weber, L.B. DaSilva, T.W. Barbee, Jr., R. Cauble, A.S. Wan, and J.C. Moreno, Opt. Letts. **20** (18), 1907 (1995).
4. M. Born and E.W olf, Principles of Optics, Chap. 7, 7th ed. (Cambridge University Press, 1999).
5. J. Dunn, R.F. Smith, J. Nilsen, J.R. Hunter, T.W. Barbee, Jr., V.N. Shlyaptsev, H. Fiedorowicz, A.Bartnik, Soft X-ray Lasers and Applications IV meeting, SPIE Proc. Vol. 4505, p.62 (2001).
6. J. Dunn et al., Journal de Physique IV (Proceedings), vol.11, (no.2), (X-Ray Lasers 2000. 7th International Conference on X-Ray Lasers, Saint-Malo, France, 19-23 June 2000.), (2001).